PAPER

Spin-dependent electrical hole extraction from low doped p-Si via the interface states in a Fe$_3$Si/p-Si structure

View the article online for updates and enhancements.

IOP ebooks™

Bringing you innovative digital publishing with leading voices to create your essential collection of books in STEM research.

Start exploring the collection - download the first chapter of every title for free.

Spin-dependent electrical hole extraction from low doped p-Si via the interface states in a Fe₃Si/p-Si structure

A S Tarasov[1,2]**, A V Lukyanenko**[1,2]**, M V Rautskii**[1] ⓘ**, I A Bondarev**[1,2] ⓘ**,
D A Smolyakov**[1]**, I A Tarasov**[1]**, I A Yakovlev**[1]**, S N Varnakov**[1]**,
S G Ovchinnikov**[1,2]**, F A Baron**[1] **and N V Volkov**[1]

[1] Kirensky Institute of Physics, Federal Research Center KSC SB RAS, Krasnoyarsk 660036, Russia
[2] Institute of Engineering Physics and Radio Electronics, Siberian Federal University, Krasnoyarsk 660041, Russia

E-mail: bia@iph.krasn.ru

Abstract

Spin accumulation effect in Fe₃Si/p-Si structure with low boron doped silicon substrate was found. Calculated spin lifetimes are comparable with results reported earlier but for structures with highly doped semiconductors (SC) with or without a tunnel barrier introduced between the SC and ferromagnet (FM). Electrical characterization of a prepared Fe₃Si/p-Si diode allowed the determination of possible reasons for the pronounced spin signal. Analysis of the forward bias I-V curve revealed a Schottky barrier at the Fe₃Si/p-Si interface with a height of $\phi_{Bp} = 0.57$ eV. Then, using impedance spectroscopy, we observed interface states localized in the band gap of silicon with energy of $E_{LS} = 40$ meV. Such states most probably cause the observed spin signal. We believe that in our experiment, spin-dependent hole extraction was performed via the interface states resulting in the minority spin accumulation in the silicon valence band. The observed effect paves the way to the development of different spintronic devices based on FM/SC structures without dielectric tunneling barriers.

Keywords: spin accumulation, interface states, hybrid structures, Hanle effect, iron silicide

(Some figures may appear in colour only in the online journal)

Introduction

The addition of spin transport to CMOS and SOI devices should lead to a new generation of devices with non-volatile memory properties, high processing speeds and high integration density [1–5]. At present, there are a large number of works on spin-dependent transport phenomena in different SC-based structures [6]. Moreover, there have been several reports on spin transistor working prototypes operated by magnetic or electric fields or by optical methods [7–10]. Carrier spin injection into a semiconductor (SC) is the first necessary condition to introduce spin degree of freedom into traditional electronics. Spin injection was demonstrated in Si [11, 12], Ge [13, 14], GaAs [15, 16] and other semi-conductors [17, 18] with various doping levels and types

using different ferromagnetic materials as injectors and dielectric films as tunneling barriers. Large scientific interest is paid to spin injectors based on ferromagnetic (FM) Heusler alloys with high spin polarization, like Fe₃Si, Co₂FeSi, Fe₂MnSi, Co₂FeAl, since they can be epitaxially grown on various semiconducting substrates [19–24]. In most of the experiments on spin injection, in order to resolve the well known problem of conductivity mismatch, three basic approaches are used, together or separately: (i) the introduction of a tunnel insulator layer between the FM metal and SC [11], (ii) heavily or degenerately doped SC wafers (10^{18} cm⁻³ carrier concentration and higher) [11, 12] and (iii) δ- doped high carrier concentration sublayers on the SC substrate surface [15, 19]. The first method directly forms a tunnel barrier, the others reduce the depletion region width in the SC to
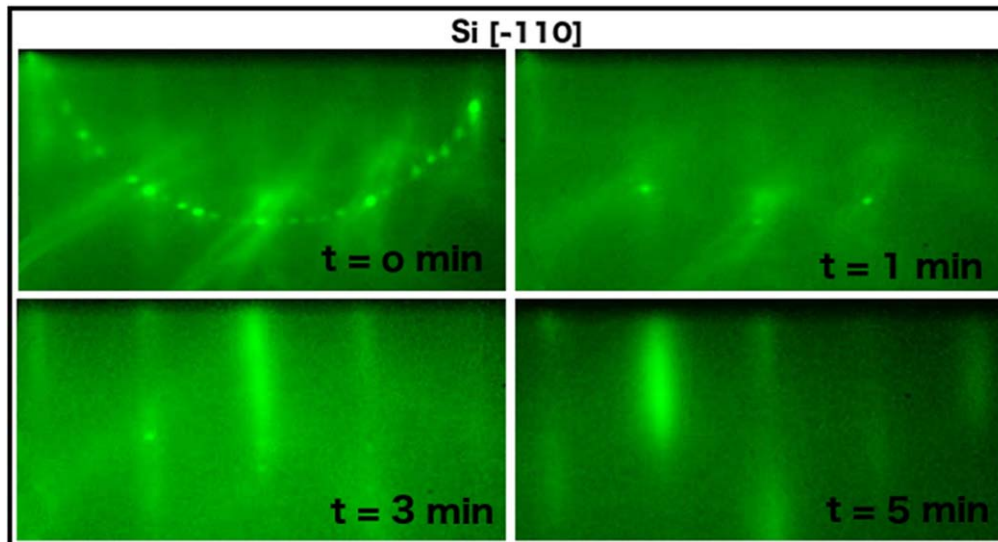
Figure 1. Evolution of experimental RHEED pattern along Si[-110] direction of Si(111) surface during the Fe$_3$Si epitaxial film growth.

increase the tunneling rate through the Schottky barrier. One of the few works devoted to studying the role of the Schottky barrier in spin injection effectiveness demonstrated the possibility of spin injection into p-type silicon with doping density as low as 10^{15} cm^{-3}, but through a tunnel SiO$_2$ layer [25]. It was shown that regardless of barrier width the localized interface states contribute to the spin-polarized electron tunneling current.

Furthermore, recent work of Rortais *et al* [26] revealed the influence of defects on electrical spin injection into silicon and germanium, and showed that defects in the dielectric layer have no significant contribution to the spin signal – a large spin signal magnitude is actually related to the presence of localized states at the MgO/Si interface. One may assume that localized interface states on the Si side can play an important role in the spin transport process in FM/insulator/SC structures. Therefore the effect of localized states and paramagnetic centers in Si requires further investigation. We believe that FM/SC structures and devices based on low doped wafers lack sufficient attention from the spin device research community. To the best of our knowledge there are no reports on spin accumulation effect measurements in low doped silicon FM/SC structures, especially for those that utilize 3- terminal Hanle (3-T) [3] or the nonlocal technique [27]. By low doping we mean lower than 10^{18} cm^{-3} carriers concentration in the semiconductor wafer or in the δ- doped layer.

In this work, we show the spin accumulation effect in an Fe$_3$Si/p-Si FM/SC structure processed using low boron doped wafers (p = 2×10^{15} cm^{-3}). Most likely the spin signal observed is due to the localized interface states, which were experimentally detected using impedance spectroscopy (IS).

Experimental details

A 50-nm-thick Fe$_3$Si epitaxial layer was grown at room temperature on moderately doped 350 μm-thick p-Si(111)

substrate with boron concentration 2×10^{15} cm^{-3} (resistivity $\rho = 7\,\Omega \cdot$ cm) by molecular beam epitaxy (MBE) in ultrahigh vacuum conditions (UHV) using a specialized MBE system described elsewhere [28]. Details of the epitaxial iron silicide synthesis technology with the DO3 structure have been described previously [29, 30]. The evolution of the RHEED pattern during the Fe$_3$Si epitaxial film growth is represented in figure 1. The RHEED pattern corresponded to the deposition time (t = 0 min) and clearly shows the presence of Si(111) 7×7 surface reconstruction. After 1 min of the deposition process (0.8 ML) the 7×7 reconstruction is absent while three spot reflections on (0$\bar{1}$), (00) and (01) streaks are still recognizable. This stage may correspond to the growth stage when the sample surface consists of the flat growing islands of the Fe$_3$Si phase and a clear Si(111)1 $\times$ 1 surface. The streak intensity increase and their broadening is easily noticeable at t = 3 min (2.5 ML) due to the increased proportion of growing silicide islands. The spot reflections disappear at a value of 4.2 ML and the RHEED pattern does not have any further different reflections. One can consider the Fe$_3$Si epitaxial thin film growth as the 3D island growth mode since at a nominal thickness higher than 1 ML the Si(111)1 $\times$ 1 reflection may be still noticed. The continuous Fe$_3$Si epitaxial film appears to be at 5 nm according to our previous research [31]. Thus, the interfacial layer may contain a higher quantity of structural defects formed during the coalescence of 3D islands than the rest of the film volume. This was confirmed earlier by the examination of an Fe$_3$Si epitaxial film with Rutherford backscattering spectrometry (RBS) channelling measurements [30]. Namely, the minimum yield χ_{min} shows increased values for the interfacial region Fe$_3$Si/Si in comparison with the main film body. Moreover, the interfacial region is usually enriched with silicon atoms due to silicon atom diffusion from the silicon substrate at elevated temperatures [32]. Thus, one may expect that the interfacial layer can demonstrate slightly different properties with respect to the main film volume due to changes in the chemical composition and chemical order [33, 34].
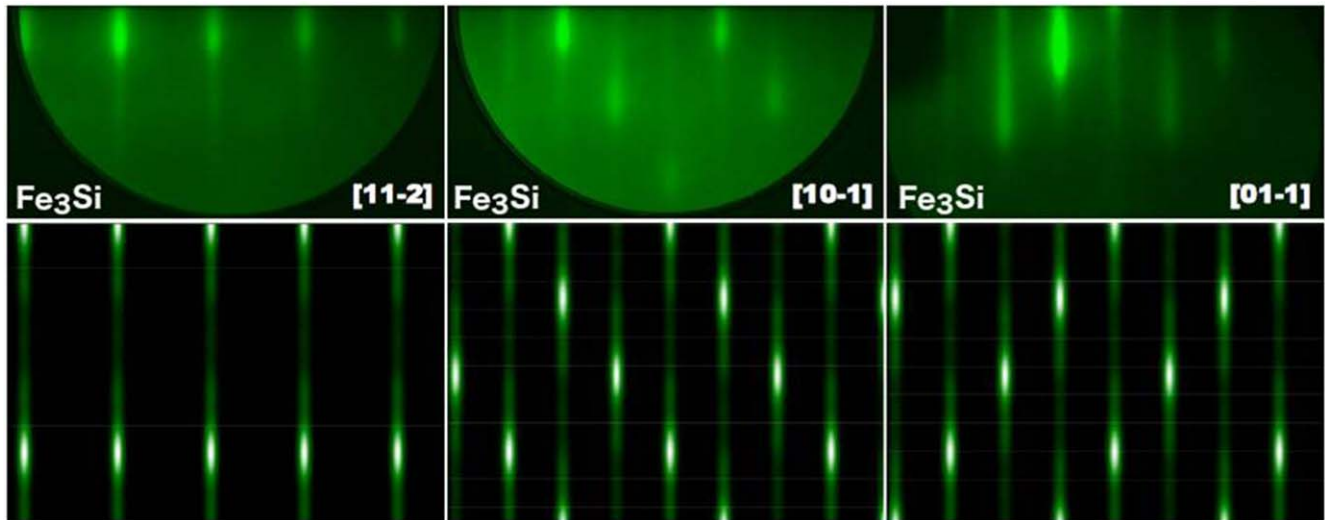
Figure 2. Upper row corresponds to experimental RHEED pattern along [11-2], [10-1] and [01-1] directions of the $Fe_3Si(111)$ surface after the growth. Lower row—simulated RHEED patterns of Fe_3Si surface along the same beam directions.
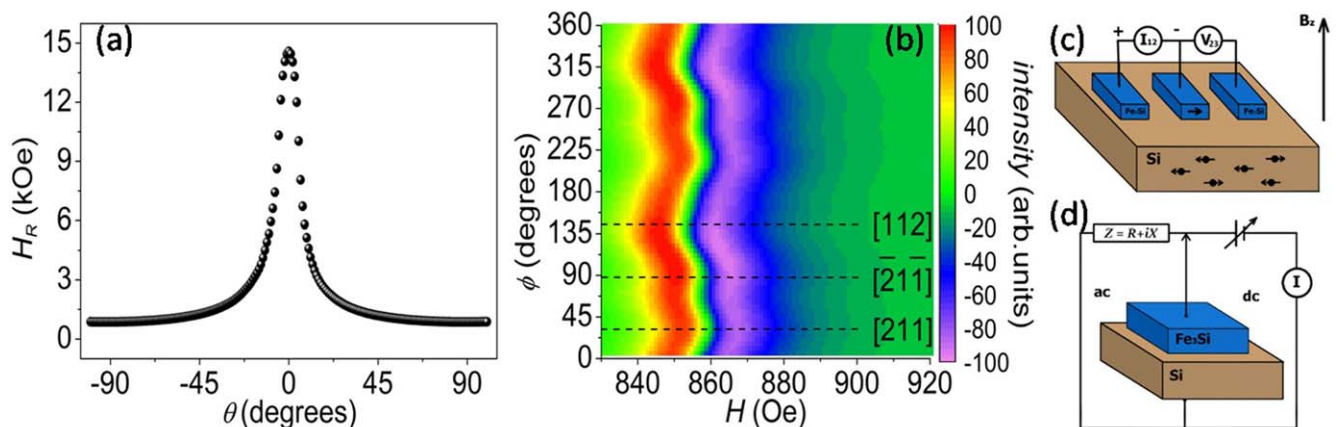

Figure 3. (a) The polar angular dependences of the resonance field H_R (out-of-plane geometry). (b) Amplitude map of azimuthal angular dependence FMR spectra (in-plane geometry). Dashed lines show the crystal orientations [112], [21-1] and [211]. Experimental schemes and sketches are shown for (c) 3-terminal planar microdevice for studying the Hanle effect and (d) Schottky diode for electrical characterization.

In order to confirm the epitaxial orientation relationship (OR) of the Fe_3Si/Si heterostrucuture the RHEED pattern of the as-grown Fe_3Si epitaxial thin film (figure 2 (upper row)) was simulated with the kinematical approach (figure 2 (lower row)), considering single electron scattering events at the surface [35]. The OR obtained is $Fe_3Si(111)[1-21]||Si(111)[11-2]$, which is consistent with our previous results [30, 36]. Moreover, the RHEED simulation approach allows us to additionally carry out an estimation of the surface roughness. It indicates the formation of islands with the length of 3 nm and three $Fe_3Si(111)$ monolayers high ($\sim$1 nm) and laying on the $Fe_3Si(111)$ surface with the coverage of 0.3 ML. The typical average roughness ($\sim$1 nm) of the Fe_3Si films measured by atomic force microscopy [30] is in agreement with the simulation results.

Polar (out-of-plane) and azimuthal (in-plane) angular dependences (at 5° angular resolution) of ferromagnetic resonance (FMR) spectra measured with the X-band (9.7 GHz) spectrometer ELEXSYS E580 (Bruker, Germany). Figure 3(a)

represents the polar angular dependences of the resonance field H_R that is defined as the H value where the derivative of P with respect to H is equal to zero: $H_R = H|_{dP/dH=0}$. Here, P is the absorbed microwave power. The maximum of H_R (14 580 Oe) corresponds to the hard magnetization axis and is observed when the external magnetic field is normal to the film plane ($\theta = 0$). The minimum of H_R (857 Oe) corresponds to the easy axis and is observed when the external magnetic field is directed within the film plane. This behavior indicates that the magnetic properties of the films are determined by shape anisotropy. Furthermore, the azimuthal angular dependence of the resonance field H_R (figure 3(b)) demonstrates the presence of crystalline anisotropy in the plane of the film. The saturation magnetization calculated from the analysis of the angular dependences of FMR resonance field amounts to 1150 emu cm^{-3}, which is close to the maximum for bulk single crystal [37] and epitaxial thin films [38–40]. The large saturation magnetization in combination with a small FMR linewidth ($\sim$17 Oe in-plane geometry) and indicates the high quality of the Fe_3Si film.
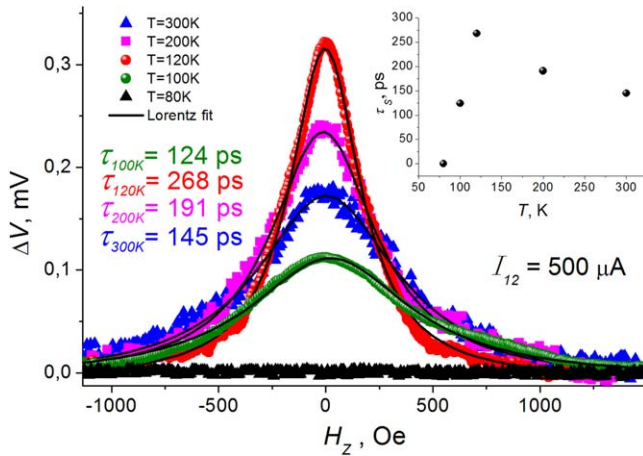
Figure 4. Hanle curves for Fe$_3$Si/p-Si device at $I_{12} = +500\ \mu$A and temperatures of 300 K, 200 K and 120 K (symbols) and Lorentzian fits (solid lines)

For 3-T measurements in Fe$_3$Si/Si structure, a 3-terminal planar micro-scale device was fabricated (figure 3(c)) using conventional photolithography process and wet chemical etching in HF: HNO$_3$: H$_2$O = 1: 2: 400 [30]. The distance between contact № 2 and contact № 3 is 10 μm. To study the Fe$_3$Si/Si interface electric properties, a diode was fabricated with an ohmic contact on the substrate backside (figure 3(d)), for which the measurements of *I-V* characteristics were performed as well as the temperature and frequency dependences of the real (Re |Z|) and imaginary (Im |Z|) parts of impedance. Studies of charge transport were performed at a cryogenic probe station Lakeshore EMPX-HF 2 and a homebuilt facility based on a helium cryostat and electromagnet [41, 42] using a Keithley 2634b SourceMeter and Agilent E4980A for dc and ac measurements, respectively, in the temperature range from 4.2 K to 300 K.

Result and discussion

Firstly, the magnetic field dependences of voltage signal ΔV_{23} were measured at a bias current $I_{12} = 500\ \mu$A using experimental geometry shown in figure 3(c). Curves for different temperatures behave similarly and have a Lorentzian shape (figure 4). It indicates the occurrence of spin accumulation under contact № 2 according to the 3-T method. Injected carrier polarization is parallel to the magnetization direction of the ferromagnetic contacts and lies in the sample plane. Out of plane magnetic field causes spin precession that results in spin accumulation suppression. Note that in the experiment, bias current I$_{12}$ was positive, i.e., contact № 2 was under negative bias. That means that the device works in a hole extraction regime. Consequently, spin accumulation is caused by spin-dependent hole extraction from silicon to Fe$_3$Si. Moreover, we observed spin signal only in the perpendicular magnetic field (as shown in figure 3(c)), i.e., direct Hanle effect. At the same time, an inverted Hanle effect [43], which is measured when a magnetic field is applied in the film plane, was not found in our structure. This effect

appears in structures with rough interfaces and is related to spin dephasing due to an inhomogeneous magnetostatic field near a ferromagnetic interface. In other words an inverted Hanle effect must be observed when a fraction of accumulated spins is oriented at a certain angle with respect to the structure plane due to the interface roughness. In this case the in-plane magnetic field should enhance the spin accumulation. Since such an effect has not been observed one may assume that the Fe$_3$Si film is very smooth.

Using the expression $\Delta V(H) = \Delta V(0)/(1 + (\omega_L \tau_s)^2)$ for the 3-T Hanle signal [11, 26] we fitted the experimental data by the Lorentzian function (figure 4). The extracted half-width of the fitting curve in its half-maximum ΔB allows for the calculation of spin lifetime $\tau_s = 1/\omega_L = h/2\pi g_h \mu_B \Delta B$, where g_h is the Lande g-factor of holes ($g_h = 2$). For our devices, experimental curve fitting yields the following values: $\tau_s = 145$ ps, 191 ps, 268 ps, and 124 ps, for $T = 300$ K, 200 K, 120 K, and 100 K, respectively. As can be seen from the inset of figure 4 the temperature dependence of the spin lifetime has a nonmonotonic behavior. Initially with decreasing temperature from 300 K to 120 K τ_s increases. Further cooling below 120 K leads to the decrease of τ_s. Furthermore, at 80 K the spin signal disappears and, consequently spin lifetime cannot be extracted from the experimental curve. At this stage of research it is difficult to give a detailed explanation or suggest mechanisms responsible for the observed temperature dependence, only some speculations can be made. Papers [44, 45] provide similar features of spin lifetime observed in n-Si and n-Ge. Ishikawa *et al* [45] shows that the temperature-dependent τ_s in Si layers originates from the temperature-dependent mobility μ and diffusion length *D*. Such an explanation may account for our results at temperatures above 120 K. Based on *Sze* [46] both μ and *D* parameters in p-Si should increase when cooling below the room temperature, consequently τ_s should also increase. However, within the framework of this simple model, the low-temperature behavior of τ_s cannot be understood. Also this effect cannot be related to any peculiar feature in the temperature dependence and specific resistance of Fe$_3$Si, which gradually decreases from room temperature down to liquid helium. This complex behavior could be related to the carrier freeze out in low-doped Si below 120 K [46] resulting in an exponential drop of holes concentration at low temperatures. Nevertheless, obtained values of the spin lifetime are comparable with other reported results for silicon-based structures probed by 3-T measurements. For example, for a structure with an epitaxial MgO(001) tunnel barrier and Fe(001) electrode τ_s in highly doped p-Si is 133 ps [47]. Previously reported [43] spin lifetime values in highly doped p-Si with Al$_2$O$_3$ tunnel barrier and different ferromagnetic electrodes were 60 ps, 110 ps and 270 ps for Fe, Co, and Ni$_{80}$Fe$_{20}$ electrodes, respectively. Another paper [19] reports $\tau_s = 470$ ps in the FM/SC structure Fe$_3$Si/n-Si with δ-doped layer with narrow width Schottky barrier. However, it is important to note that in our case the spin injection occurred into the low doped wafer with relatively high resistivity ($p = 2 \times 10^{15}$ cm^{-3}, $\rho = 7\ \Omega \cdot$ cm). Moreover, our Fe$_3$Si/p-Si structure did not contain a tunnel insulator layer between FM and SC. According to the standard spin diffusion model [48], those two circumstances create a mismatch
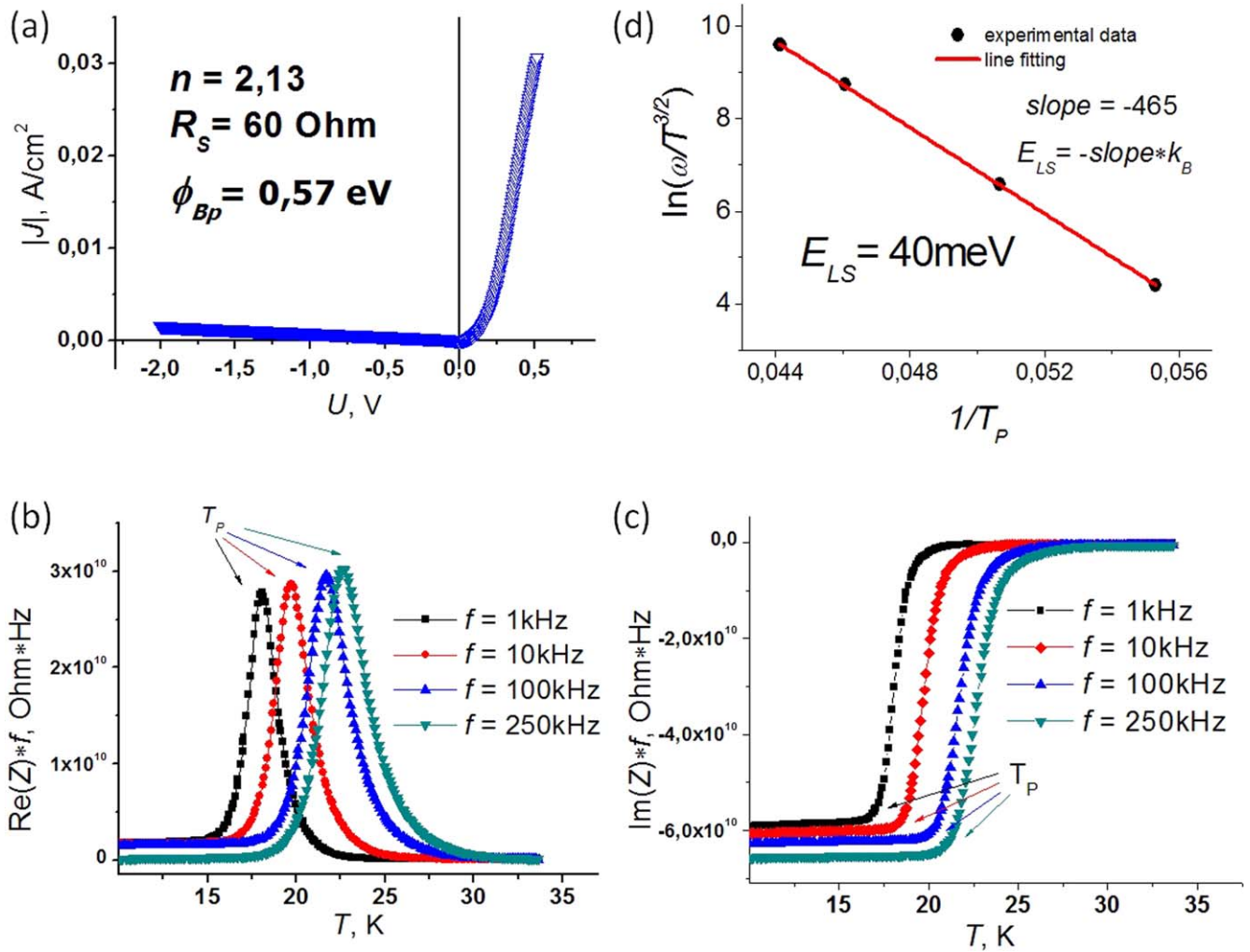
Figure 5. (a) *I–V* curve of the Fe_3Si/p-Si Schottky diode at 295 K. Temperature dependences of normalized (b) active and (c) reactive resistances at different frequencies. (d) $\ln(\omega/T_P^{3/2})$ versus $1/T_P$ plot allows calculating energy of localized states E_{LS}.

conductivity problem which should have strongly reduced the spin signal. So, let us explore the reasons why the spin accumulation effect was quite pronounced in our device.

First of all, for spin injection into a highly resistive Si interface, resistance should be significant. For the FM/SC structure, the Schottky barrier could provide such a high resistance. We measured the *I-V* characteristics of a specially prepared Fe_3Si/p-Si diode and found that the curves demonstrate rectifying behavior (figure 5(a)) which indicates the presence of the Schottky barrier. Indeed, analysis of the forward bias *I-V* curve by Cheung's method [49] revealed a Schottky barrier at the Fe_3Si/p-Si interface, with height $\phi_{Bp} = 0.57$ eV. However, for silicon with $2 \times 10^{15}\,cm^{-3}$ doping the depletion region width is about 700 nm [50], and such a barrier has a very small tunneling rate. In this case, the charge transport may occur due to the charge transfer over the barrier by thermionic emission. Therefore, the presence of the Schottky barrier in our structure can hardly be the sole cause of the spin-dependent transport effect.

The work of Dankert *et al* [25] reported efficient spin injection into silicon through a 736-nm-wide Schottky barrier and tunneling SiO_2 layer simultaneously. Authors considered

the mechanism of spin injection by tunneling via interface states, the model of which was suggested earlier [51]. However, there were no attempts to detect such states, for example, by optical or electrical spectroscopy techniques. Assuming that in our structure there might be various surface and interface states that most likely caused the observed spin signal, we tried to detect them using impedance spectroscopy (IS) [52–54]. By this technique one could measure the thermal emission rate in the space-charge region located very close to the crossing point of the Fermi level with the energy level of states localized near the insulator/semiconductor interface. A search of the crossing point was carried out by temperature scanning during the IS experiment that induced movement of the Fermi level within the forbidden band.

For the same Fe_3Si/p-Si diode, temperature dependences of the real and imaginary parts of impedance were measured (figures 5(b) and (c)). At low temperatures, we observed a sharp peak on the resistance curve and the peak temperature position T_P is frequency-dependent. This indicates the presence of a thermally activated energy state. This state charge-discharges under the action of ac voltage bringing up peaks and step features on the frequency and temperature plots of ac
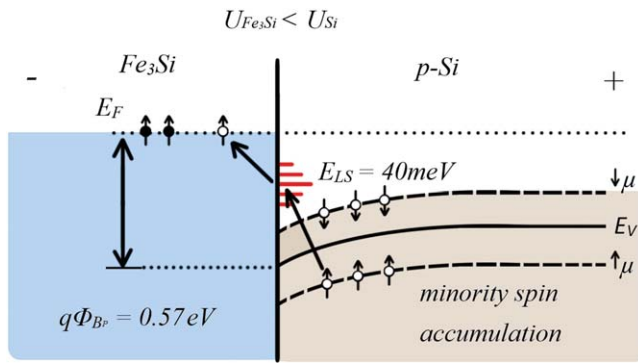
Figure 6. Schematic energy-band diagram depicting spin-polarized holes transport through the Fe$_3$Si/p-Si junction via localized interface states assisted tunneling.

resistance, reactance, admittance or impedance. One can estimate the state energy using the following expression for the recharging rate: $\langle \omega \rangle = 2C\, N_V \exp(-E_{LS}/k_B T)\beta^{-1}$ [52]. Here $\omega = 2\pi f$ is the angular frequency of the applied ac voltage, C is the capture coefficient, k_B is the Boltzman constant and β is the degeneracy factor. Since the valence-band density of states $N_V(T) \sim T^{3/2}$ one can extract the energy of localized states E_{LS} from the slope of $\ln(\omega/T_P{}^{3/2})$ versus $1/T_P$. We obtained $E_{LS} = 40$ meV for the extracted value of T_P observed at frequencies from 1 kHz to 250 kHz (figure 5(d)). Such low energy means that detected states can participate in dc transport processes even at room temperature. Assuming the presence of a $\phi_{Bp} = 0.57$ eV Schottky barrier and localized interface states in our structure, we can construct the energy band diagram and propose a scheme of spin-polarized holes transport (figure 6). As mentioned above, contact № 2 was under negative bias (figure 3(c)), i.e. our device worked in spin extraction regime. Holes from the valence band tunnel via localized states into the Fe$_3$Si electrode. The tunneling probability of spin polarized carriers depends on the density of states (DOS) of the corresponding spin subbands $D\uparrow(E_F)$ and $D\downarrow(E_F)$ in the ferromagnetic electrode. Initially both spin polarizations of holes in the silicon valence band have equal DOS. However, since in Fe$_3$Si electrode spin up $D\uparrow(E_F)$ and spin down $D\downarrow(E_F)$ subbands DOS are different, the hole transport from Si to Fe$_3$Si becomes spin polarized. If Fe$_3$Si is spin up polarized, i.e. $D\uparrow(E_F) - D\downarrow(E_F) > 0$, then the spin up transport channel prevails. We believe that as a result of the spin up polarized holes extraction there occurs the spin accumulation of holes with spin down direction in the silicon valence band, i.e. minority spin accumulation. This process is highlighted in figure 6. In reality the spin down holes also take part in the transport but the probability of this process is much lower. It is worth mentioning the possibility of energy levels splitting the localized states. Thus formed spin subbands would also have different tunneling probabilities. Another important requirement for the two step tunneling to take place is the availability of unoccupied localized states at the interface. We believe that the low values of energy E_{LS} extracted from our IS data is a strong indication that, indeed, such sates are empty within the temperature range in our 3T-Hanle

experiment. Unfortunately at this stage of our research studies it is hard to elucidate the nature of these states. Perhaps they are formed at the initial stage of the film growth process.

Another possible reason for the sharp spin signal is extremely high spin polarization of the ferromagnetic contact. On the one hand, the spin polarization of the ideal structurally and chemically ordered DO$_3$ Fe$_3$Si is about 50% [55]. On the other hand, Karel *et al* [34] calculated DOS and theoretically showed that the spin polarization can change from -12% to 77% due to variations of the chemical order in the Fe$_{0.65}$Si$_{0.35}$ compound. The strong dependence of Fe magnetic moment on the nearest-neighbor environment of iron in Fe$_3$Si and Fe$_x$Si$_{1-x}$ compounds was shown in work of Zamkova *et al* [56]. Therefore, it can be assumed that Fe$_3$Si in our structure has an imperfect chemical order DO$_3$ (this is also indicated by XRD data [36]) which leads to an increase of the spin polarization above 50%. However the 100% spin polarization condition is likely not satisfied in our structure and it is needed to circumvent the conductivity mismatch problem allowing barrier-free diffusive spin transport. Still using the proposed scheme of the interface states-assisted tunneling in conjunction with Fe$_3$Si highly spin polarized electrodes may deliver higher spin injection efficiency than other structures containing simple 3d ferromagnetic metals like Fe or Co.

Conclusions

Spin accumulation in low doped p-Si with epitaxial Fe$_3$Si film was studied using the 3-T Hanle method. The room temperature spin lifetime $\tau_s = 145$ ps was extracted from the voltage versus magnetic field Lorentzian curves. The obtained data is in good agreement with other reported results for silicon-based devices. However, according to the standard spin diffusion model, our structure should not demonstrate a spin accumulation effect due to the high resistivity of the substrate, which is the reason why most of the spin injection experiments with the SC transport use channels with high carrier concentration. We proposed several reasons that explain the experimental data. Most probably, the pronounced spin signal was due to the presence of localized interface states at the Fe$_3$Si/Si interface. This suggestion is supported by impedance spectroscopy (IS) measurements. Within the framework of our model IS revealed the interface states with energy $E_{IS} = 40$ meV above the valence band edge in silicon. Thus, we suggest that spin-dependent transport between Fe$_3$Si and p-Si was realized via the interface states, which led to minority spin accumulation in the silicon valance band. Observed at room temperature this giant spin accumulation phenomenon indicates that it may become possible to create spintronic devices based on FM/SC structures without dielectric tunneling barriers. We believe that our experimental findings may help develop a deeper understanding of spin transport phenomena in FM/SC structures.

Acknowledgments

ORCID iDs

M V Rautskii ⬡ https://orcid.org/0000-0002-5346-6125
I A Bondarev ⬡ https://orcid.org/0000-0001-8155-3958

References

[1] Sato K, Saitoh E, Willoughby A, Capper P and Kasap S (ed) 2015 *Spintronics for Next Generation Innovative Devices* (New York: Wiley) Chap. 10

[2] Nikonov D E and Young I A 2013 Overview of beyond-CMOS devices and a uniform methodology for their benchmarking *Proc. IEEE* V **101** I: 12

[3] Jansen R, Dash S P, Sharma S and Min B C 2012 Silicon spintronics with ferromagnetic tunnel devices *Semicond. Sci. Technol.* **27** 083001

[4] Žutić I, Fabian J and Sarma S D 2004 Spintronics: Fundamentals and applications *Rev. Mod. Phys.* **76** 323

[5] Žutić I, Fabian J and Erwin S C 2006 Spin injection and detection in silicon *Phys. Rev. Lett.* **97** 026602

[6] Txoperena O and Casanova F 2016 Spin injection and local magnetoresistance effects in three-terminal devices *J. Phys. D: Appl. Phys.* **49** 133001

[7] Chuang P *et al* 2015 All-electric all-semiconductor spin field-effect transistors *Nat. Nanotechnol.* **10** 35–9

[8] Koo H C, Kwon J H, Eom J, Chang J, Han S H and Johnson M 2009 Control of spin precession in a spin-injected field effect transistor *Science* **325** 1515–8

[9] Wunderlich J, Park B-G, Irvine A C, Zârbo L P, Rozkotová E, Nemec P, Novák V, Sinova J and Jungwirth T 2010 Spin Hall effect transistor *Science* **330** 1801–4

[10] Tahara T, Koike H, Kameno M, Sasaki T, Ando Y, Tanaka K, Miwa S, Suzuki Y and Shiraishi M 2015 Room-temperature operation of Si spin MOSFET with high on/off spin signal ratio *Appl. Phys. Express* **8** 113004

[11] Dash S P, Sharma S, Patel R S, de Jong M P and Jansen R 2009 Electrical creation of spin polarization in silicon at room temperature *Nature* **462** 491

[12] Sharma S, Spiesser A, Dash S P, Iba S, Watanabe S, van Wees B J, Saito H, Yuasa S and Jansen R 2014 Anomalous scaling of spin accumulation in ferromagnetic tunnel devices with silicon and germanium *Phys. Rev. B* **89** 075301

[13] Fischer I A, Chang L T, Sürgers C, Rolseth E, Reiter S, Stefanov S, Chiussi S, Tang J, Wang K L and Schulze J 2014 Hanle-effect measurements of spin injection from $Mn_5Ge_3C_{0.8}/Al_2O_3$-contacts into degenerately doped Ge channels on Si *Appl. Phys. Lett.* **105** 222408

[14] Iba S, Saito H, Spiesser A, Watanabe S, Jansen R, Yuasa S and Ando K 2012 Spin accumulation and spin lifetime in p-type germanium at room temperature *Applied Physics Express* **5** 053004

[15] Tran M, Jaffrès H, Deranlot C, George J M, Fert A, Miard A and Lemaître A 2009 Enhancement of the spin accumulation at the interface between a spin-polarized tunnel junction and a semiconductor *Phys. Rev. Lett.* **102** 036601

[16] Misuraca J, Kim J I, Lu J, Meng K, Chen L, Yu X, Zhao J, Xiong P and von Molnár S 2014 Bias current dependence of the spin lifetime in insulating $Al_{0.3}Ga_{0.7}As$ *Appl. Phys. Lett.* **104** 082405

[17] Jahangir S, Doğan F, Kum H, Manchon A and Bhattacharya P 2012 Spin diffusion in bulk GaN measured with MnAs spin injector *Phys. Rev. B* **86** 035315

[18] Han W, Jiang X, Kajdos A, Yang S H, Stemmer S and Parkin S S 2013 Spin injection and detection in lanthanum- and niobium-doped $SrTiO_3$ using the Hanle technique *Nat. Commun.* **4** 2134

[19] Fujita Y, Yamada S, Ando Y, Sawano K, Itoh H, Miyao M and Hamaya K 2013 Room-temperature sign reversed spin accumulation signals in silicon-based devices using an atomically smooth Fe3Si/Si (111) contact *J. Appl. Phys.* **113** 013916

[20] Kawano M, Santo K, Ikawa M, Yamada S, Kanashima T and Hamaya K 2016 Spin transport in p-Ge through a vertically stacked Ge/Fe3Si junction *Appl. Phys. Lett.* **109** 022406

[21] Kasahara K, Fujita Y, Yamada S, Sawano K, Miyao M and Hamaya K 2014 Greatly enhanced generation efficiency of pure spin currents in Ge using Heusler compound Co_2FeSi electrodes *Applied Physics Express* **7** 033002

[22] Yamada M, Tsukahara M, Fujita Y, Naito T, Yamada S, Sawano K and Hamaya K 2017 Room-temperature spin transport in n-Ge probed by four-terminal nonlocal measurements *Applied Physics Express* **10** 093001

[23] Yamada S, Honda S, Hirayama J, Kawano M, Santo K, Tanikawa K, Kanashima T, Itoh H and Hamaya K 2016 Magnetic properties and interfacial characteristics of all-epitaxial Heusler-compound stacking structures *Phys. Rev. B* **94** 094435

[24] Sakai S, Kawano M, Ikawa M, Sato H, Yamada S and Hamaya K 2017 Low-temperature growth of fully epitaxial CoFe/Ge/Fe3Si layers on Si for vertical-type semiconductor spintronic devices *Semicond. Sci. Technol.* **32** 094005

[25] Dankert A, Dulal R S and Dash S P 2013 Efficient spin injection into silicon and the role of the Schottky barrier *Sci. Rep.* **3** 3196

[26] Rortais F, Vergnaud C, Ducruet C, Beigné C, Marty A, Attané J P, Widiez J, Jaffrès H, George J-M and Jamet M 2016 Electrical spin injection in silicon and the role of defects *Phys. Rev. B* **94** 174426

[27] Sasaki T, Suzuki T, Ando Y, Koike H, Oikawa T, Suzuki Y and Shiraishi M 2014 Local magnetoresistance in Fe/MgO/Si lateral spin valve at room temperature *Appl. Phys. Lett.* **104** 052404

[28] Varnakov S N, Lepeshev A A, Ovchinnikov S G, Parshin A S, Korshunov M M and Nevoral P 2004 Automation of technological equipment for obtaining multilayer structures in an ultrahigh vacuum *Instruments and Experimental Techniques* **47** 839–43

[29] Yakovlev I A, Varnakov S N, Belyaev B A, Zharkov S M, Molokeev M S, Tarasov I A and Ovchinnikov S G 2014 Study of the structural and magnetic characteristics of epitaxial Fe3Si/Si (111) films *JETP Lett.* **99** 527–30

[30] Tarasov A S *et al* 2017 Approach to form planar structures based on epitaxial $Fe_{1-x}Si_x$ films grown on Si (111) *Thin Solid Films* **642** 20–4

[31] Tarasov I A, Popov Z I, Varnakov S N, Molokeev M S, Fedorov A S, Yakovlev I A, Fedorov D A and Ovchinnikov S G 2014 Optical characteristics of an epitaxial Fe₃Si/Si(111) iron silicide film *JETP Lett.* **99** 565

[32] Oki S, Yamada S, Tanikawa K, Yamasaki K, Miyao M and Hamaya K 2013 Lateral spin valves with two-different Heusler-alloy electrodes on the same platform *Appl. Phys. Lett.* **103** 212402

[33] Tarasov I, Popov Z, Visotin M, Yakovlev I and Varnakov S 2018 Effect of chemical ordering on optical properties of Fe₃Si epitaxial films *EPJ Web Conf.* **185** 03014

[34] Karel J *et al* 2015 Effect of chemical order on the magnetic and electronic properties of epitaxial off-stoichiometry Fe$_x$Si$_{1-x}$ thin films *Phys. Rev.* B **91** 144402

[35] Wang K and Smith A R 2011 Efficient kinematical simulation of reflection high-energy electron diffraction streak patterns for crystal surfaces *Comput. Phys. Commun.* **182** 2208–12

[36] Sandalov I, Zamkova N, Zhandun V, Tarasov I, Varnakov S, Yakovlev I, Solovyov L and Ovchinnikov S 2015 Effect of electron correlations on the Fe₃Si and $\alpha-$FeSi₂ band structure and optical properties *Phys. Rev.* B **92** 205129

[37] Hines W A, Menotti A H, Budnick J I, Burch T J, Litrenta T, Niculescu V and Raj K 1976 Magnetization studies of binary and ternary alloys based on Fe₃Si *Phys. Rev.* B **13** 4060

[38] Yamada S, Sagar J, Honda S, Lari L, Takemoto G, Itoh H, Hirohata A, Mibu K, Miyao M and Hamaya K 2012 Room-temperature structural ordering of a Heusler compound Fe₃Si *Phys. Rev.* B **86** 174406

[39] Lenz K, Kosubek E, Baberschke K, Wende H, Herfort J, Schönherr H P and Ploog K H 2005 Magnetic properties of Fe₃Si/GaAs (001) hybrid structures *Phys. Rev.* B **72** 144411

[40] Herfort J, Schönherr H P and Ploog K H 2003 Epitaxial growth of Fe₃Si/GaAs (001) hybrid structures *Appl. Phys. Lett.* **83** 3912–4

[41] Volkov N V, Tarasov A S, Eremin E V, Eremin A V, Varnakov S N and Ovchinnikov S G 2012 Frequency-dependent magnetotransport phenomena in a hybrid Fe/SiO₂/p-Si structure *J. Appl. Phys.* **112** 123906

[42] Volkov N V, Tarasov A S, Smolyakov D A, Gustaitsev A O, Rautskii M V, Lukyanenko A V, Volochaev M N, Varnakov S N, Yakovlev I A and Ovchinnikov S G 2017 Extremely high magnetic-field sensitivity of charge transport in the Mn/SiO₂/p-Si hybrid structure *AIP Adv.* **7** 015206

[43] Dash S P, Sharma S, Le Breton J C, Peiro J, Jaffrès H, George J-M, Lemaître A and Jansen R 2011 Spin precession and inverted Hanle effect in a semiconductor near a finite-roughness ferromagnetic interface *Phys. Rev.* B **84** 054410

[44] Hamaya K, Baba Y, Takemoto G, Kasahara K, Yamada S, Sawano K and Miyao M 2013 Qualitative study of temperature-dependent spin signals in n-Ge-based lateral devices with Fe₃Si/n-Ge Schottky-tunnel contacts *J. Appl. Phys.* **113** 183713

[45] Ishikawa M, Oka T, Fujita Y, Sugiyama H, Saito Y and Hamaya K 2017 Spin relaxation through lateral spin transport in heavily doped n-type silicon *Phys. Rev.* B **95** 115302

[46] Sze S M and Ng K K 2006 *Physics of Semiconductor Devices* (New York: John Wiley & Sons) p 30 ISBN: 0-471-05661-8

[47] Spiesser A, Sharma S, Saito H, Jansen R, Yuasa S and Ando K 2012 Electrical spin injection in p-type Si using Fe/MgO contacts *In Spintronics* V vol 8461, p 84610K*Int. Society for Optics and Photonics*

[48] Fert A and Jaffres H 2001 Conditions for efficient spin injection from a ferromagnetic metal into a semiconductor *Phys. Rev.* B **64** 184420

[49] Cheung S K and Cheung N W 1986 Extraction of Schottky diode parameters from forward current-voltage characteristics *Appl. Phys. Lett.* **49** 85–7

[50] Sze S M and Ng K K 2006 *Physics of Semiconductor Devices* (New York: John Wiley & Sons) p 84

[51] Jansen R, Deac A M, Saito H and Yuasa S 2012 Injection and detection of spin in a semiconductor by tunneling via interface states *Phys. Rev.* B **85** 134420

[52] Losee D L 1975 Admittance spectroscopy of impurity levels in Schottky barriers *J. Appl. Phys.* **46** 2204–14

[53] Dueñas S, Izpura I, Arias J, Enriquez L and Barbolla J 1991 Characterization of the DX centers in AlGaAs: Si by admittance spectroscopy *J. Appl. Phys.* **69** 4300–5

[54] Volkov N V, Tarasov A S, Smolyakov D A, Gustaitsev A O, Balashev V V and Korobtsov V V 2014 The bias-controlled giant magnetoimpedance effect caused by the interface states in a metal-insulator-semiconductor structure with the Schottky barrier *Appl. Phys. Lett.* **104** 222406

[55] Kudrnovský J, Christensen N E and Andersen O K 1991 Electronic structures and magnetic moments of Fe$_{3+y}$Si$_{1-y}$ and Fe$_{3-x}$VxSi alloys with DO3-derived structure *Phys. Rev.* B **43** 5924

[56] Zamkova N G, Zhandun V S, Ovchinnikov S G and Sandalov I S 2017 Effect of local environment on moment formation in iron silicides *J. Alloys Compd.* **695** 1213–22